Simultaneous observations of the auroral ovals in both hemispheres under varying conditions

T. J. Stubbs,[1] R. R. Vondrak,[1] N. Østgaard,[2,3] J. B. Sigwarth,[1,4] and L. A. Frank[5]

[1] This is the first analysis to use simultaneous observations of the entire auroral ovals in both hemispheres to track their location. Data was used from the Polar VIS and IMAGE FUV imagers on 23 October 2002 and plotted in AACGM coordinates. Results showed the expected IMF B_y-dependent asymmetry along the dawn-dusk meridian; however, there was an unexpected offset of both ovals toward dawn. Evidence is also shown for an asymmetry along the noon-midnight meridian dependent on both dipole tilt angle and the sense of IMF B_x. During a brief period of weak IMF $B_z > 0$ and IMF $B_x > 0$, the southern oval is observed to move equatorward relative to the northern oval, consistent with tail lobe reconnection occurring only in the southern hemisphere. This has important implications for the global response of the magnetosphere to different interplanetary conditions. **Citation:** Stubbs, T. J., R. R. Vondrak, N. Østgaard, J. B. Sigwarth, and L. A. Frank (2005), Simultaneous observations of the auroral ovals in both hemispheres under varying conditions, *Geophys. Res. Lett.*, *32*, L03103, doi:10.1029/2004GL021199.

1. Introduction

[2] Recently, it has been possible to simultaneously observe the entire auroral ovals in the northern and southern hemispheres with imagers aboard the IMAGE and Polar spacecraft, respectively. We use this unprecedented opportunity to investigate inter-hemispheric asymmetries – and therefore the global response of the magnetosphere to changes in the interplanetary magnetic field (IMF) – by tracking the location of the main auroral ovals. *Craven et al.* [1991] reported the first simultaneous observations of the entire auroral ovals in both hemispheres, but their study focused on transpolar arcs and not the main ovals. The IMAGE FUV-SI13 camera observes OI emissions at 135.6 nm [*Mende et al.*, 2000]; while the VIS Earth camera (VIS-EC) is sensitive in the range from 124 to 149 nm, which is dominated by OI emissions at 130.4 and 135.6 nm [*Frank and Sigwarth*, 2003]. Therefore, the auroral forms observed in the far ultra-violet (FUV) with these instruments are comparable [*Østgaard et al.*, 2003].

[1]Laboratory for Extraterrestrial Physics, NASA Goddard Space Flight Center, Greenbelt, Maryland, USA.
[2]Space Sciences Laboratory, University of California, Berkeley, California, USA.
[3]Now at Department of Physics and Technology, University of Bergen, Bergen, Norway.
[4]Formerly at Department of Physics and Astronomy, University of Iowa, Iowa City, Iowa, USA.
[5]Department of Physics and Astronomy, University of Iowa, Iowa City, Iowa, USA.

[3] *Cowley et al.* [1991] have argued that the orientation of the IMF controls the location of the auroral ovals via an "effective" partial penetration into the closed magnetosphere. In the northern hemisphere the oval is predicted to shift toward dawn (dusk) for IMF $B_y > 0$ ($B_y < 0$), and predicted to shift toward midnight (noon) for IMF $B_x > 0$ ($B_x < 0$). The oval in the southern hemisphere is predicted to shift in the opposite sense, thereby causing an inter-hemispheric asymmetry. *Holzworth and Meng* [1984] analyzed 130 DMSP auroral images at magnetically quiet times, where $\approx 1/4$ of the oval was visible, with hour-averaged IMF data. Their results indicated that IMF B_y controlled the location of the ovals along both the dawn-dusk and the noon-midnight meridians, with a $\approx 2.5°$ inter-hemispheric displacement along each meridian between periods of IMF $B_y \approx \pm 4$ nT. However, *Cowley et al.* [1991] suggested that the noon-midnight result could have been detecting the IMF B_x effect described above, due to the strong anti-correlation in the sense of IMF B_x and B_y (a consequence of the average Parker spiral IMF). Also, *Oznovich et al.* [1993] showed that dipole tilt angle, Ψ, controls the location of the northern oval by shifting it toward midnight (noon) for $\Psi > 0$ ($\Psi < 0$) at the rate of $\approx 1°$ per $10°$ change in Ψ. Here Ψ is defined as the angle between the magnetic axis and the GSM Z-axis, such that $\Psi > 0$ ($\Psi < 0$) is toward (away from) the Sun.

[4] In order to track the position of an auroral oval we determine its "centroid" by fitting an offset circle to the average auroral latitude weighted by brightness, $\langle \theta \rangle_{kR}$, as shown in Figure 1. ($\langle \theta \rangle_{kR} = \sum \theta . A / \sum A$, where θ is latitude and A is brightness.) $\langle \theta \rangle_{kR}$ is calculated every 0.5 hrs of MLT over a narrow band of latitudes (determined using the previous circle fit to the oval), as well as above a minimum brightness threshold. This minimizes contributions from non-auroral and background brightness. The data is plotted as a function of altitude-adjusted corrected geomagnetic (AACGM) latitude and MLT [*Baker and Wing*, 1989], so the fitted circle is offset from the magnetic pole. Note that the automated fitting routine fits a circle to the main oval, as observed at all MLTs, which minimizes distortion from auroral features within the oval, such as substorms. *Holzworth and Meng* [1984], and references therein, showed that the main oval could be well approximated by a circle. Here we use this circle fitting technique to test the above theories relating to the IMF and dipole tilt dependence of the location of the auroral ovals.

2. Observations

[5] Figure 2 shows a selection of near-simultaneous images of the entire auroral ovals in the northern (left) and southern (right) hemispheres, observed between 11:24 and 12:10 UT on 23 October 2002 by IMAGE FUV-SI13 and Polar VIS-EC, respectively. In both sets of images typically
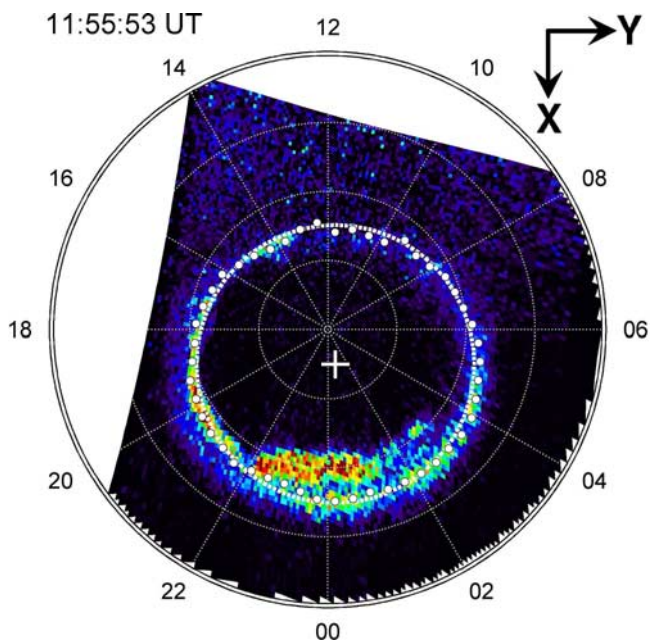
Figure 1. Example of an offset circle (broken white line) fitted to the main auroral oval for an FUV-SI13 image. The white dots represent the average auroral latitude weighted by brightness, and the white cross indicates the "centroid" of the oval.

≈80% of the dayglow caused by solar FUV has been removed, thus revealing a band of dayside aurora. The white dots show the location of the geographic poles. In these images we can immediately identify the near-circular main oval at all MLT, as well as the progression of a substorm near midnight. The main oval in the north appears near-symmetric about the noon-midnight meridian, with the substorm activity occurring about 00 MLT. In the south, however, the oval is noticeably displaced toward dawn, and substorm activity is shifted toward dusk taking place about 23 MLT.

[6] Figure 3 shows the IMF conditions for this event with the auroral centroid positions, radii and errors from the circle fitting routines. The IMF data in Figures 3a–3c are plotted in GSM coordinates, and were obtained from the Geotail MGF magnetometer while it was just upstream of the bow shock. The IMF propagation time to the Earth (X = 0) of ≈7.5–8 minutes was calculated using CPI plasma data and the technique described by *Stubbs et al.* [2004]. There is an additional time-shift of Δt = +10 minutes to account for the auroral response time along the noon-midnight meridian [see *Cowley and Lockwood*, 1992, and references therein]. In Figures 3d–3g the solid green lines and the broken red lines show the northern (FUV-SI13) and southern (VIS-EC) ovals, respectively, with dots indicating the times when images were acquired. Figures 3d and 3e show the positions of the auroral centroids relative to the magnetic pole along the noon-midnight (X_0) and dawn-dusk (Y_0) meridians, respectively. As shown by the axes in Figure 1, midnight and dawn are in the positive directions. The radial extent of the ovals (R_0), as determined from the circle fitting, is shown in Figure 3f. In Figure 3g we show the standard deviations of Δr ($\sigma_{\Delta r}$), where Δr is the difference between $\langle\theta\rangle_{kR}$ and the circle fit, which gives an indication of how well the circle fit represents the auroral
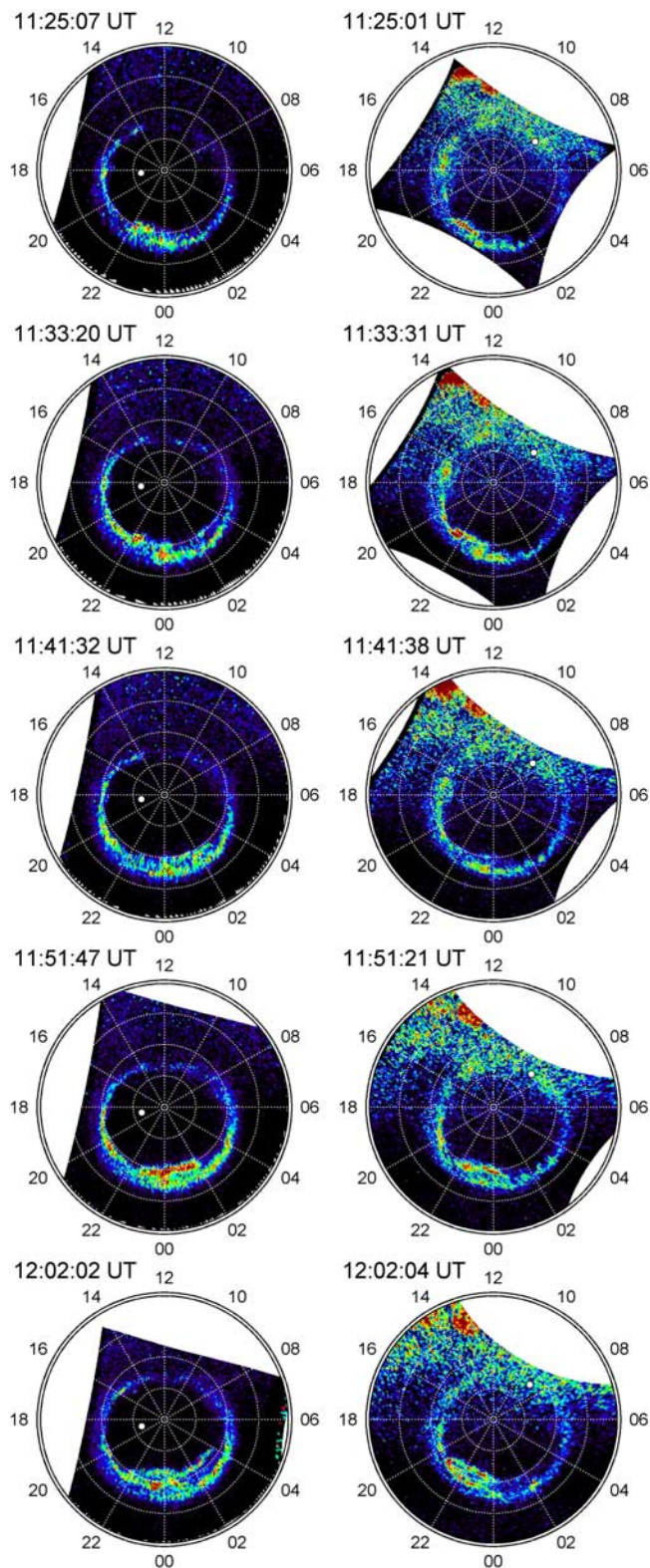
Figure 2. Series of near-simultaneous auroral images observed between 11:24 and 12:10 UT on 23 October 2002. Observations were made of the northern (left) and southern (right) hemispheres by FUV-SI13 and VIS-EC, respectively. White dots indicate the geographic poles.
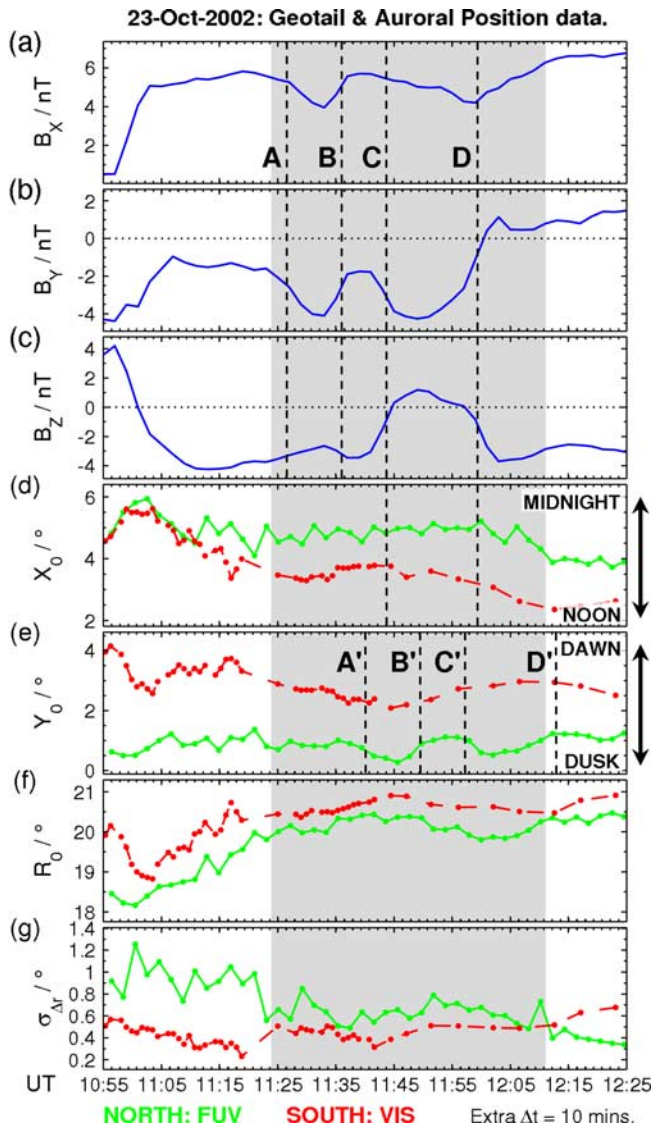
Figure 3. Panels (a) to (c) show the IMF X, Y and Z components in GSM coordinates, time-shifted to account for the lag to the Earth and the noon-midnight auroral response time, Δt. Panels (d) to (f) show the circle fit results: with X_0 and Y_0 showing the auroral centroid locations along the AACGM noon-midnight and dawn-dusk meridians, respectively; and R_0 indicating the radial extent of the ovals. The locations of the northern (FUV-SI13) and southern (VIS-EC) ovals are shown by the green solid and red broken lines respectively. Panel (g) shows the standard deviations ($\sigma_{\Delta r}$) of the circle fits.

oval. The gray shading in Figure 3 indicates the interval from 11:24 to 12:10 UT when both ovals could be observed simultaneously at all MLT, and hence when the circle fitting routine is most reliable. Changes in the IMF that can be related to shifts in the location of the auroral ovals are marked by vertical dashed lines at times A, B, C and D.

[7] During the entire interval both ovals are shifted toward midnight, as shown in Figure 3d, which is consistent with the distortion of the Earth's magnetic field caused by solar wind dynamic pressure. Even so, the northern oval is consistently over $1°$ closer to midnight than the southern

oval. During this period $\Psi \approx -8°$, so from *Oznovich et al.* [1993] we would expect the southern oval to be $\approx 1.5°$ closer to midnight. Although, from the *Cowley et al.* [1991] interpretation of the *Holzworth and Meng* [1984] results, we might expect the partial penetration of the coincident IMF $B_x \approx 5$ nT to shift the northern oval further toward midnight by $\approx 2.5°$. However, from a combination of these two effects we could expect the northern oval to be further toward midnight than the southern oval by $\approx 1°$, as is observed. During the interval of IMF $B_z > 0$, between times C and D, the ovals appear to diverge with the southern oval moving almost $1°$ closer to noon. Following time D both ovals move toward noon; this is consistent with the closure of open flux in the magnetotail, as evidenced by the substorm activity shown in Figure 2, and reconnection at the dayside magnetopause caused by the southward turning of the IMF.

[8] From Figure 3e we can see that during the entire interval there was an offset of both ovals toward dawn, which is quite unexpected. (Results from *Holzworth and Meng* [1984] tended to show an offset toward dusk, although this was not commented upon.) In addition, the two ovals are offset relative to each other by between $1.5°$ and $2.5°$, with the southern oval dawnward of the northern oval. This is again consistent with the partial penetration of IMF B_y varying between ≈ -2 and -4 nT. In fact, the changes seen in IMF B_y at times A, B, C, and D are consistent with the changes seen along Y_0 in the northern oval at times A′, B′, C′, and D′. These changes were not seen so clearly in the southern oval, possibly due to either the lower VIS-EC image rate at this time, or uncertainties in the circle fitting routines. As expected, the extent of the ovals, shown in Figure 3f, is similar to within $\approx 0.5°$. Although the variations in the position of the ovals are at times of order $\approx 1°$, which is close to the uncertainties in the circle fitting routine shown in Figure 3g, during the periods of greatest interest the uncertainties are smaller. The con-
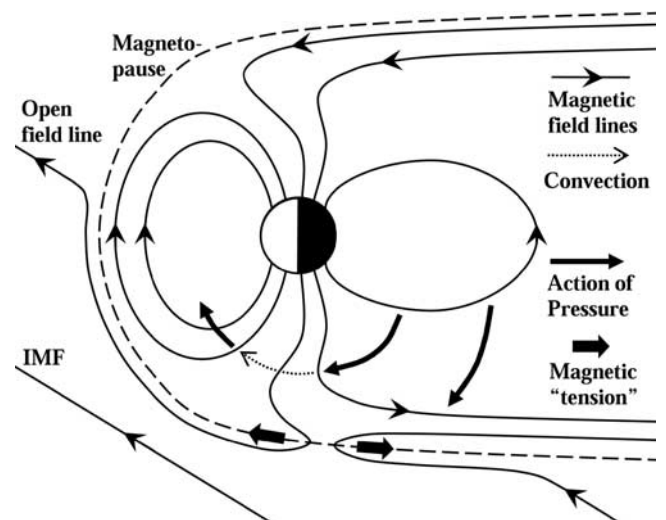
Figure 4. Schematic (not to scale) showing the effect on the magnetosphere of the interval of weak IMF $B_z > 0$ and IMF $B_x > 0$ (from time C to D), when tail lobe reconnection occurs preferentially in the southern hemisphere. Open flux is convected from the tail toward the dayside (indicated by the dotted arrowed line), causing the southern oval to shift toward noon.

sistency of the features in the data that we have commented upon suggests that we have identified genuine trends in the relative locations of the auroral ovals.

3. Discussion

[9]   From the interpretation in section 2, the results appear to be consistent with previously observed dipole tilt and IMF-related effects. However, we interpret the motion of the southern oval toward noon between times C and D as being caused by magnetopause reconnection occurring preferentially at the southern tail lobe due to a highly inclined IMF, i.e., $\tan(B_z/B_x) \approx 11°$, and $\Psi \approx -8°$. As illustrated in Figure 4, we suggest that following tail lobe reconnection open flux is convected toward the dayside, as indicated by the dotted arrowed line. This transfer of open flux from the tail to the dayside magnetosphere, and the associated pressure (thick black arrowed lines) acting to attain a new equilibrium state [*Cowley and Lockwood*, 1992], causes the southern oval to shift toward noon. The open field lines generated by tail lobe reconnection will eventually be carried anti-sunward by the solar wind flow once the magnetic tension acting on them relaxes. During the interval of southward IMF, prior to time C, open flux accumulates in the tail due to dayside reconnection. Between times C and D, when the IMF turns northward, evidence for the re-closing of open flux in the tail is shown in Figure 3f by both ovals shrinking during this period, and by the substorm activity shown in Figure 2.

[10]   From Figure 3 we notice that there was a longer response time of the ovals along the dawn-dusk meridian ($\approx$20 mins) than along the noon-midnight meridian ($\approx$10 mins). We suggest that this was because of the more direct transfer of electromagnetic stresses along the noon-midnight meridian due to the solar wind flow being primarily aligned in that direction. Responding to changes along the dawn-dusk meridian takes longer since it requires the excitation of ionospheric flows transverse to the solar wind flow direction in order for the magnetosphere to reach a new equilibrium state [*Cowley and Lockwood*, 1992].

[11]   The cause of the offset of both ovals toward dawn, as shown in Figure 3e, is not immediately obvious. For this interval, the pointing of FUV-SI13 was based on a comparison with star positions and was accurate to <70 km; while the pointing of VIS-EC was based on a comparison with the limb of the Earth and was accurate to <50 km. So the maximum pointing errors were <0.5°, which was much less than the observed >2° dawn offset. The 130.4 and 135.6 nm emissions observed by VIS-EC and FUV-SI13 had different optical thicknesses. However, since both imagers were viewing from near nadir, the uncertainties ($\sim$10 km) were much less than the spatial resolution of the imagers ($\sim$50 km). Therefore, we suggest that the different offsets of the geographic pole from the magnetic pole, shown in Figure 2, caused by the non-dipolar components of the Earth's magnetic field contributed to this global feature. Initial comparisons with various empirical magnetic field models have so far failed to reproduce the dawnward offset. In order to understand this we must study additional events under a variety of conditions.

4.   Summary

[12]   We have presented the first analysis to use simultaneous observations of the entire auroral ovals from both hemispheres in order to track their location. The results were consistent with the predictions of *Cowley et al.* [1991] that an effective partial penetration of IMF B_x and B_y creates inter-hemispheric asymmetries along the noon-midnight and dawn-dusk meridians respectively. We have also shown that these observations are qualitatively consistent with some of the results of *Holzworth and Meng* [1984] relating to IMF effects, and with the dipole tilt angle dependence identified by *Oznovich et al.* [1993].

[13]   In the observations presented here there was an unexpected offset of both auroral ovals toward dawn. This was not caused by FUV-SI13 or VIS-EC pointing errors. Initial comparisons with various empirical magnetic field models have not appeared to resolve this issue. We suggest that this may be related to the non-dipolar component of the Earth's magnetic field; however, additional events need to be studied in order to better understand this result.

[14]   We also present evidence that reconnection at the tail lobe magnetopause can occur in one hemisphere and not in the other when IMF $|B_x| \gg |B_z|$, as was observed here. In this case, reconnection occurred only in the southern hemisphere causing the southern oval to move toward noon as a result of the redistribution of open flux and pressure balance within the magnetosphere, as illustrated in Figure 4.

References

Baker, K. B., and S. Wing (1989), A new magnetic coordinate system for conjugate studies at high-latitudes, *J. Geophys. Res.*, *94*, 9139–9143.

Cowley, S. W. H., and M. Lockwood (1992), Excitation and decay of solar wind-driven flows in the magnetosphere-ionosphere system, *Ann. Geophys.*, *10*, 103–115.

Cowley, S. W. H., J. P. Morelli, and M. Lockwood (1991), Dependence of convective flows and particle precipitation in the high-latitude dayside ionosphere and the X and Y components of the interplanetary magnetic field, *J. Geophys. Res.*, *96*, 5557–5564.

Craven, J. D., J. S. Murphree, L. A. Frank, and L. L. Cogger (1991), Simultaneous optical observations of transpolar arcs in the two polar caps, *Geophys. Res. Lett.*, *18*, 2297–2300.

Frank, L. A., and J. B. Sigwarth (2003), Simultaneous images of the northern and southern auroras from the Polar spacecraft: An auroral substorm, *J. Geophys. Res.*, *108*(A4), 8015, doi:10.1029/2002JA009356.

Holzworth, R. H., and C.-I. Meng (1984), Auroral boundary variations and the interplanetary magnetic field, *Planet. Space Sci.*, *32*, 25–29.

Mende, S. B., et al. (2000), Far ultraviolet imaging from the IMAGE spacecraft: 3. Spectral imaging of Lyman- and OI 135.6 nm, *Space Sci. Rev.*, *91*, 287–318.

Østgaard, N., S. B. Mende, H. U. Frey, L. A. Frank, and J. B. Sigwarth (2003), Observations of non-conjugate theta aurora, *Geophys. Res. Lett.*, *30*(21), 2125, doi:10.1029/2003GL017914.

Oznovich, I., R. W. Eastes, R. E. Huffman, M. Tur, and I. Glaser (1993), The aurora at quiet magnetospheric conditions: Repeatability and dipole tilt angle dependence, *J. Geophys. Res.*, *98*, 3789–3797.

Stubbs, T. J., P. J. Cargill, M. Lockwood, M. Grande, B. J. Kellett, and C. H. Perry (2004), Extended cusp-like regions and their dependence on the Polar orbit, seasonal variations, and interplanetary conditions, *J. Geophys. Res.*, *109*, A09210, doi:10.1029/2003JA010163.

————————

L. A. Frank, Department of Physics and Astronomy, University of Iowa, Iowa City, IA 52242–1479, USA.

N. Østgaard, Department of Physics and Technology, University of Bergen, N-5007 Bergen, Norway.

J. B. Sigwarth, T. J. Stubbs, and R. R. Vondrak, NASA Goddard Space Flight Center, Mail Code 690.4, Greenbelt, MD 20771, USA. (tstubbs@lepvax.gsfc.nasa.gov)